HYPERGOLIC IGNITION OF CATALYTICALLY PROMOTED FUELS WITH ROCKET HYDROGEN PEROXIDE

W.E. Anderson, T.L. Pourpoint
Purdue University – School of Aeronautics and Astronautics, West Lafayette, United-States

Ignition of hypergolic propellants is generally described according to Semenov's theory of thermal ignition. For the case of reaction between hydrogen peroxide and a fuel loaded with a catalyst, however, no general model exists. Measured ignition delays of hydrogen peroxide and fuel/catalyst mixtures are reported herein. Test parameters included hydrogen peroxide concentrations and ambient pressure. A physical model of the ignition of these quasi-hypergols is presented. The model and the experimental results are used to postulate a 2nd order ignition reaction consistent with conventional theory for thermal ignition.

Background

The ignition delay of a given fuel / oxidizer combination can be defined as the observed difference between the time at which the fuel and the oxidizer come into contact and the time at which they ignite. This global ignition delay can be further divided into the physical delay and the chemical delay. The chemical delay is the interval separating the start of the chemical reaction and the initiation of a flame. The physical delay is then the difference between the global delay and the chemical delay. The physical delay is mostly influenced by the physical properties of the propellants: viscosity, surface tension, and miscibility. The chemical delay is determined by the reaction potential of the two propellants.

The three ignition delays are shown in fig. 1 for a drop-on-drop ignition test and an impinging jet test with Rocket Grade Hydrogen Peroxide (RGHP) and a catalytically promoted fuel ('Block 0') consisting of manganese acetate tetrahydrate dissolved in methanol. In fig. 1, adapted from a schematic of Barrère and Moutet [1], the reaction zone temperature is plotted as a function of time from the start of the injection process. Assuming miscible liquid propellants the segment *OA* represents the contact time in liquid phase, or the physical delay. During this time the temperature does not increase and no chemical reaction can be seen. After instant *A* an exothermic reaction starts in liquid phase and increases the mixture tempera-

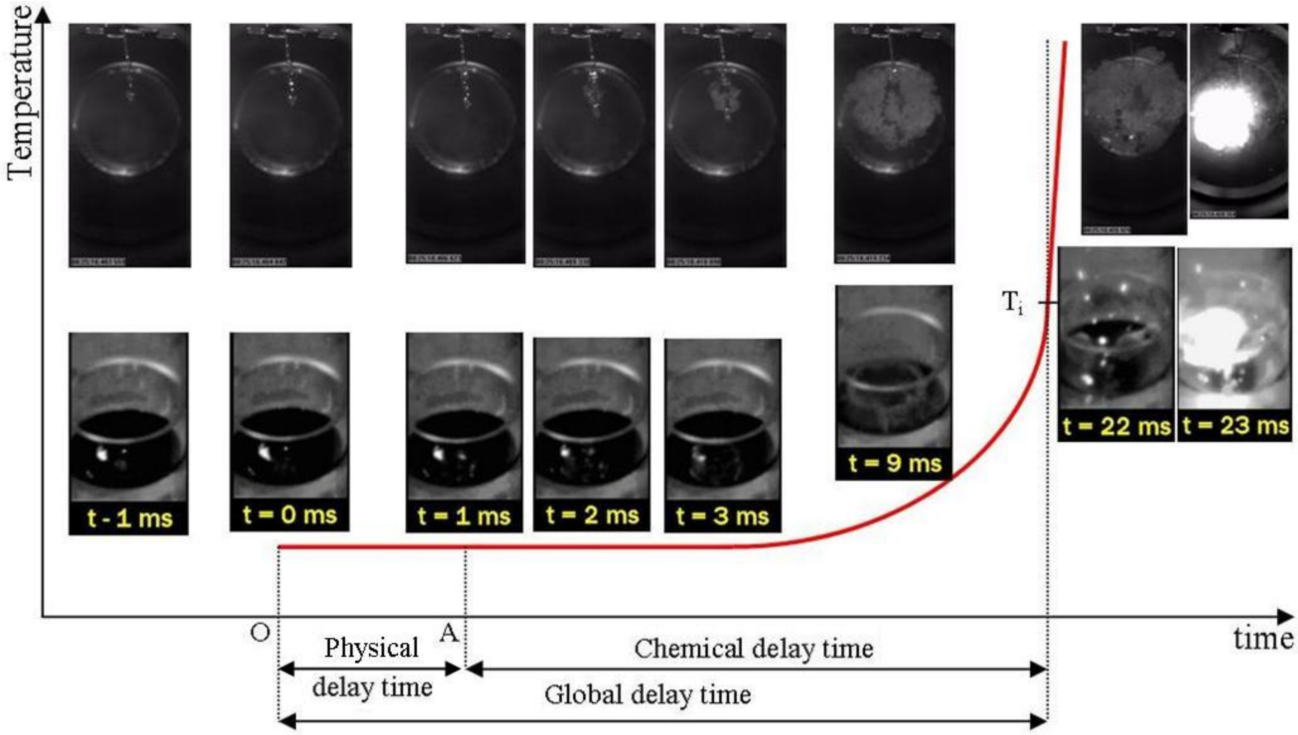

Fig. 1

ture to the ignition temperature, T_i. At that temperature, the reaction rate increases exponentially according to the Arrhenius equation. It is supposed that this reaction occurs in the vapor phase.

Thermal Ignition Theory

Arrhenius' Law of Reaction Rate Constant

The dependence of chemical reaction velocities on temperature is most satisfactorily expressed by the empirical correlation attributed to Arrhenius. Assuming that the ignition delay, τ, of a fuel-oxidant reaction may be taken as a given fractional completion of the reaction at a given pressure, the integrated form of the Arrhenius equation is

$$\tau = A' e^{\frac{E}{RT}} \qquad (1)$$

Since visible signs of incipient chemical reactions can be difficult to identify, it is somewhat surprising that Eq. (1) is found to hold for many fuel-oxidant reactions [2]. There is no precise definition for the transition between liquid diffusion and liquid reaction. For example, the start of the chemical delay may be defined by the chemical bubbling at the propellant surface, or as the first appearance of smoke. The start of the chemical delay time from visual observation is also somewhat subjective. It is therefore crucial to define a clear criterion for identifying ignition delays.

In the case of the reaction between RGHP and catalytically loaded hypergolic fuels, it is generally observed that the physical delay time is less than 5% of the total ignition delay time. This can be verified from the time scale shown in fig. 1. Furthermore, the instant in time at which the fuel and oxidizer impinge on each other can be precisely and non-subjectively determined by observation of high speed video footages. The accuracy of the ignition delay determination depends in this case on the maximum frame rate of the high speed camera.

Semenov's Theory of Thermal Ignition

The principles of the thermal ignition phenomenon were first quantitatively explained by Semenov, a Russian scientist whose contributions to the combustion and molecular physics fields are often acknowledged. According to Semenov's theory of thermal ignition, autoignition is possible if the heat generated by the preignition reactions equals or exceeds the heat lost to the surrounding medium [3, 4]. The theory assumes that thermal effects rather than chain branching govern the chemical reactions.

Semenov considered a chemical reaction between well-mixed, vapor-phase reactants. The temperature is assumed constant and uniform across the system. The walls of the system and the external temperature are assumed equal to be the ambient temperature T_0.

At the critical point, or ignition threshold, the heat generation and heat loss curve are tangential. We can therefore derive a relationship between pressure, temperature and composition by solving the following system of equations.

$$\begin{cases} \left.\dot{q}_{gen}\right)_c = \left.\dot{q}_{loss}\right)_c \\ \left.\left(\dfrac{d\dot{q}_{gen}}{dT}\right)\right._c = \left.\left(\dfrac{d\dot{q}_{loss}}{dT}\right)\right._c \end{cases} \tag{2}$$

Considering a vessel of volume V and surface S, the rate at which heat is generated by the chemical reaction, $\dot{q}_{gen}$, is given by

$$\dot{q}_{gen} = -V\left(\Delta H \frac{dC}{dt}\right) \tag{3}$$

Assuming an initial mixture with two species (a and b) and that the reaction rate, dC/dt, follows the conventional Arrhenius exponential law, equation (3) can be modified to

$$\dot{q}_{gen} = V\Delta H\left(AC_a^{n_a}C_b^{n_b}\exp\left(\frac{-E}{RT_{mix}}\right)\right) \tag{4}$$

The rate at which heat is lost to the surroundings, $\dot{q}_{loss}$, is given by

$$\dot{q}_{loss} = hS(T_c - T_0) \tag{5}$$

The system of equations thus becomes

$$\begin{cases} \Delta HVAC_{ac}^{n_a}C_{bc}^{n_b}e^{-E/RT_c} = hS(T_c - T_0) \\ \Delta HVAC_{ac}^{n_a}C_{bc}^{n_b}e^{-E/RT_c}\dfrac{E}{RT_c^2} = hS \end{cases} \tag{6}$$

Assuming a negligible amount of reactant consumed during the ignition delay, Eq. (6) can be simplified to a quadratic equation

$$\frac{RT_c^2}{E} = (T_c - T_0) \tag{7}$$

with two roots of the form

$$T_c = \frac{E}{2R} \pm \frac{E}{2R}\sqrt{1 - \frac{4RT_0}{E}} \tag{8}$$

As mentioned by Kanury [3], the lower root applies to ignition and the upper one to extinction. Following Kanury's derivation, it can easily be shown that, typically, the critical temperature, T_c, can be approximated by the initial temperature T_0 with minimal error. Assuming T_0 equal to the adiabatic decomposition temperature of 99% H_2O_2 and an activation energy of 20,000 cal/mol, the error is of the order of 15%. This error is deemed acceptable for the purposes of the present study.

Using Eq. (7) to rewrite the first equation in the system (6), we get

$$\Delta HVAC_{ac}^{n_a}C_{bc}^{n_b}e^{-E/RT_c} = hS\frac{RT_c^2}{E} \tag{9}$$

Assuming species a and b are perfect gases, Eq. (9) becomes

$$\Delta HVAX_{ac}^{n_a}X_{bc}^{n_b}\left(\frac{P_c}{RT_c}\right)^{n_a+n_b}e^{-E/RT_c} = hS\frac{RT_c^2}{E} \tag{10}$$

Reorganizing and taking the log of both sides of Eq. (10) gives Semenov's equation for an n^{th} order thermal reaction

$$\ln\left(\frac{P_c}{T_c^{n+2/n}}\right) = \ln\left(\frac{hSR^{n+1}}{\Delta HVAX_{ac}^{n_a} X_{bc}^{n_b} E}\right) + \frac{E}{nRT_c} \quad (11)$$

Plotting $\ln(P_c/T_c^{(n+2)/n})$ on versus $1/T_c$ should give a straight line with a slope of $E/(nR)$.

Assuming a known reaction order and a good estimate of the critical temperature, the ignition limits of the reaction between RGHP and Block 0 lead to a simple determination of the activation energy.

The reaction between RGHP and Block 0 leads to the very rapid decomposition of the RGHP; decomposition generates superheated water vapor and oxygen

$$2H_2O_{2(l)} \rightarrow 2H_2O_{(l)} + O_{2(g)} + 2884\ \text{kJ/kg} \quad (12)$$

For these propellants, the decomposition process is triggered by the reaction of the RGHP with the MnO_2 colloids in suspension in the fuel. Multiple ignition delay tests such as those shown on fig. 1 have shown that the delay required for the decomposition process to start is a fraction of the total delay time. It is postulated that during the remainder of the ignition delay period the heat generated by the decomposition process is absorbed by the fuel droplets which in turn vaporize. Ignition occurs if enough thermal energy is generated to heat the fuel above its autoignition temperature. If this thermal energy exchange is indeed the governing process for the ignition of catalytically promoted fuels with RGHP, then it may be assumed that the adiabatic decomposition temperature of RHGP has a significant effect on ignition delay.

The propagation of heat in the reaction zone is also influenced by the ambient pressure. The heat generation term given by Eq. 4 can be conveniently rewritten by replacing the species concentrations by the product of the total density ρ and the mass fraction ε of the reacting species. Equation (4) then becomes

$$\dot{q}_{gen} = V\Delta H\left(A\rho^n \varepsilon^n \exp\left(\frac{-E}{RT_{mix}}\right)\right) \quad (13)$$

The heat release is therefore a function of pressure through the density term. The heat loss term is a less sensitive function of pressure through the convective heat transfer coefficient. The conventional conclusion that ignition delays decrease with increasing initial ambient pressure should thus be verified [4]. Furthermore, since heat generation increases with pressure, it can be expected that the effect of the initial RGHP concentration (and thus the adiabatic decomposition temperature) will diminish with increasing pressure. Following Semenov's analysis, the ignition delay values obtained with different hydrogen peroxide concentration should asymptotically reach a common value as pressure increases.

Ignition Delay Experiments

Experimental Setup

A series of experiments was performed with an experimental device in which a jet of fuel impinged on a jet of RGHP. The remotely operated system is structured around a cylindrical combustion chamber. The chamber can be connected to a vacuum pump or a pressurization system for ignition tests at initial pressures ranging from 50 torr to 3 atm.

The propellants were stored in large reservoirs located upstream of the run valves. The tanks were oversized compare to the volume of propellants loaded to ensure a uniform pressure load during the test firings. Over-sized pneumatically actuated ball valves were used as the run valves to ensure that full flow conditions were achieved quickly. The propellant feed lines were sized to ensure minimum pressure drops while keeping the fill time as low as possible. Propellant feed lines were primed prior to testing.

Originally designed as a combustion bomb, the chamber (see fig. 2) is a stainless steel vessel that is 19 cm tall and 30 cm wide. The walls are 3.7 cm thick leaving an internal volume of approximately 8.7 liters. Four evenly distributed access ports on the chamber periphery were used for the injector assembly housing, optical grade windows, and to drain the chamber from combustion residues at the end of each test. The chamber is mounted vertically on the test stand with the injector pointing downwards (see fig. 3). The temperature and pressure inside the combustion chamber are monitored by means of K-type thermocouples and a pressure transducer connected to a data acquisition system.

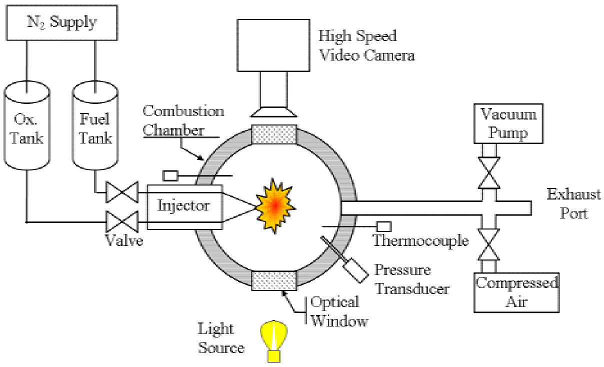

Fig. 2

The injector assembly is made entirely out of stainless steel. It consists of five plates assembled to position two spray nozzles. The oxidizer spray tip orifice diameter is approximately equal to 0.686 mm. It is 15% larger than the fuel orifice diameter (≈ 0.584 mm) in order to achieve a mixture ratio at the impingement point as close as possible to the stoichiometric mixture ratio while maintaining reasonable momentum and momentum flux ratios. The injection velocities are typically between 7 and 9 m/s. In accordance with previous hypergolic studies, it was decided to set the included angle between the jets at 60 deg to provide optimum mixing [5]. The propellant tanks, the instrumented combustion chamber, and the high speed video camera are shown on fig. 4.

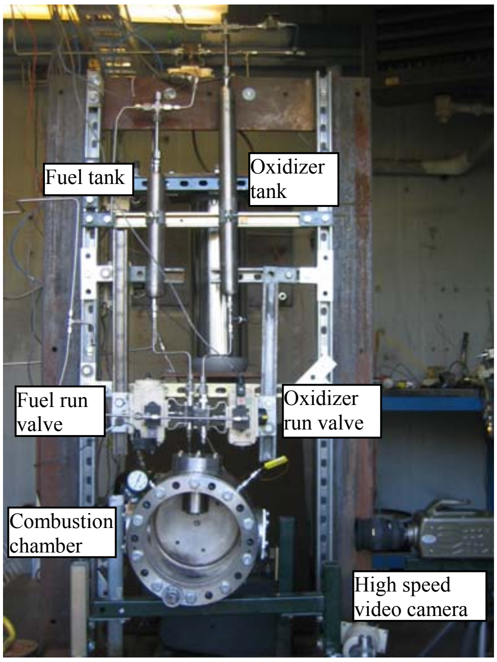

Fig. 3

Impinging Jets Experimental Results

A total of 264 tests were performed to study the influence of initial ambient pressure and RGHP concentration on the ignition delay times of Block 0. Concentrations of 99%, 96.4%, and 94% were investigated to provide a significant range of decomposition temperatures. Four distinct regions were defined for the initial ambient pressure. Region 1 comprised the sub-atmospheric pressure tests, region 2 included tests at atmospheric conditions, and regions 3 and 4 included pressures ranging from 1.8 to 2.2 atm and from 2.5 to 2.9 atm respectively.

Ignition delay values were obtained from high speed videos of the events at 10,000 frames/s. The ignition delay values were calculated by subtracting the time at which the two jets crossed each other from the time at which light is emitted from the ignition site. Table 1 summarizes the number of tests ran for each concentration and the percentage of tests with ignition delay (τ) below 100, 60, and 30 ms.

Table 1

Ignition Delay Tests Statistics

Concentration	Percent of Total Tests			
	Total Number	$\tau < 100$ ms	$\tau < 60$ ms	$\tau < 30$ ms
94 %	95	28 %	26 %	9 %
96.4 %	84	38 %	31 %	18 %
99 %	85	61 %	49 %	27%

As can be seen from Table 1, the percentage of tests with long ignition delay values increases with decreasing hydrogen peroxide concentration. While less than a third of the tests performed with 94% RGHP have ignition delay values below 100 ms, the percentage goes up to about 60% with 99% RGHP. It is therefore evident that concentration has a strong effect on ignition delay.

The small percentage of tests with short ignition delays can be attributed to non-ideal test conditions. For example, it was observed in several cases that the synchronization of the valve opening had a strong effect on jet stability; a short delay in opening the valve would cause the leading jet to oscillate upon actuation of the second valve. This is attributed to the vibrations induced by the pneumatic actuator. In other cases, air bubbles trapped inside the injector caused the jets to breakup almost immediately after exiting the spray tips. Subsequent reactions between the fuel and the oxidizer would start inside a cloud of droplets, leading to ignition delays that were difficult to measure and, generally, much greater than in the desired case of two liquid jets impinging on each other.

For these reasons, a criterion was defined to set the lowest acceptable ignition delay value. A careful examination of the high speed videos revealed that, upon exiting the injector, the jets travel about 7.6 cm inside the combustion chamber in approximately 30 ms. Since the distance between the jet impingement point and the bottom of the chamber is 15.2 cm, it takes approximately 60 ms for the first droplets to hit the chamber floor. Assuming that the fuel and the oxidizer drops hit the floor at the same time and allowing 10 ms for those drops to react, an ignition delay criterion of 70 ms was set. With the criterion, percentages of useable ignition delay values are 28%, 34%, and 52% for 94%, 96.4% and 99% RGHP, respectively.

Ignition delay values below 70 ms for all three concentrations and all test pressures are shown in fig. 4.

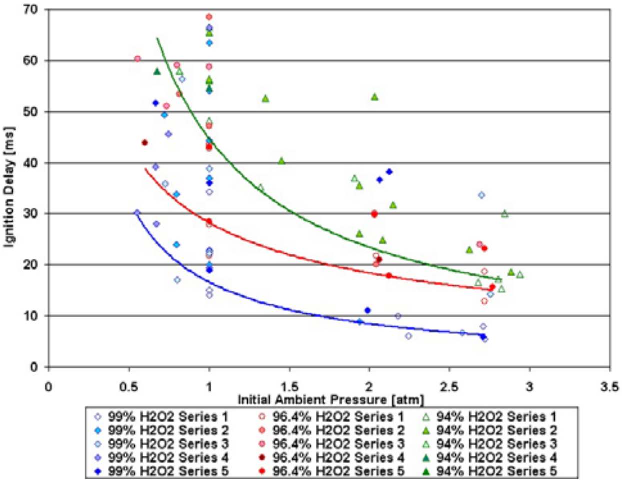

Fig. 4

The trendlines were calculated using the minimum ignition delay values for each concentration. The equations and coefficient of determinations, r^2, of the trendlines are given in Table 2.

Table 2

Ignition Delay Trendlines

Concentration	Equation (τ in ms, P in atm)	r^2
94 %	$\tau = 44.71(P)^{-0.932}$	0.972
96.4 %	$\tau = 28.29(P)^{-0.621}$	0.842
99 %	$\tau = 16.63(P)^{-0.974}$	0.925

The correlations given in Table 2 have high correlation coefficients. Such values are indicative of the strong role of pressure in the ignition processes between hydrogen peroxide and a catalytically promoted fuel.

As a first approximation, the pressure exponents in Table 2 can be related to the reaction order since the half-life of a n^{th} order chemical reaction is proportional to pressure raised to the power (1-n) and, similarly the half-life, the ignition delay is characteristic of the progress of a reaction. Using the best two correlations of Table 2, the reaction order is approximately 1.9.

Recalling Semenov's equation (Eq. 11) and assuming a 2^{nd} order reaction between RGHP and Block 0, a plot of $ln(P_c/T_c^2)$ versus $1/T_c$ can be obtained (fig.6). The critical temperature is assumed equal to the adiabatic decomposition temperature of hydrogen peroxide. The critical pressures are assumed equal to the lowest pressures at which valid ignition delay values ($\tau \leq 70$ ms) were obtained. Due to the discrete nature of the pressures that were investigated, it was decided to use the two lowest pressures for each concentration.

As shown in fig. 6, the slope of the linear interpolation is equal to 4571 which, for a second order reaction, leads to a pseudo activation energy of 18,165 cal/mol. Since the activation energy value obtained depends on the choice of temperature in Semenov's equation and since the critical temperature is likely to be lower than the adiabatic decomposition temperature of RGHP, the value given above is only indicative of the magnitude of the true activation energy.

As shown by the error bars of fig. 5, the data points are within ±5% of the interpolation line. This is a relatively large uncertainty considering the limited number of data points. It is concluded that more data points are needed at low initial ambient pressures.

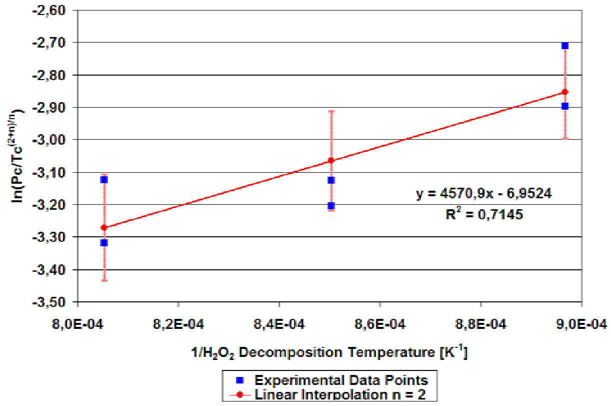

Fig. 5

Conclusions

Analysis of experimental data demonstrates that initial ambient pressure and hydrogen peroxide concentration have a significant effect on the ignition delay of a catalytically promoted fuel. Ignition delays obtained with three distinct hydrogen peroxide concentrations decrease and reach a common value as initial chamber pressure increases. These observations are in agreement with thermal ignition theories. However, the relative variations in active species concentrations with ambient pressure and hydrogen peroxide concentrations should also be considered.

References

[1] Barrère M and Moutet A. Inflammation et allumage dans les moteurs-fusées à propergols liquides. *Selected Combustion Problems, II.* Butterworths Scientific Publications, 1956.

[2] Mullins B.P. *Spontaneous ignition of liquid fuels*. Butterworths Scientific Publications, 1955.

[3] Kanury A.M. *Introduction to combustion phenomena*. Gordon and Breach, Science Publishers, Inc., 1977.

[4] Hurlbert E.A. and Moreland R.J. Propellant ignition and flame propagation. *Second International Symposium on Liquid Rocket Propulsion*. Chatillon France, June 19-21, 1995.

[5] Gill G.S. and Nurick W.H. Liquid Rocket Engine Injectors. *NASA SP-8089*. National Technical Information Service. March 1976.